Stable charge states and half-metallic ferromagnetic ordering in Fe-doped diamond

E M Benecha[1] **and E B Lombardi**
Department of Physics, University of South Africa, P.O Box 392, UNISA 003, Pretoria, South Africa

E-mail: ebenecha@gmail.com

Abstract. Half-metallic ferromagnetic semiconductors are of considerable interest for the injection and transport of spin polarised currents necessary for spintronic device development. We report *ab initio* pseudopotential DFT calculations on the magnetic ordering properties of Fe-doped diamond and show that half-metallic ferromagnetic ordering can be achieved in diamond – which is a well known material for its extreme properties – by incorporating Fe^{+1} at the substitutional lattice site. We show that substitutional Fe^{+1} possesses a magnetic moment of 1.0 μ_B per atom, and a large ferromagnetic stabilization energy of 33 meV, with the Fermi level crossing bands for only the spin-up orientation. We predict substitutional Fe^{+1} to be the most stable form of Fe in *p*-type boron doped diamond; co-doping with boron is likely to further increase the spin charge concentration.

1. Introduction

Half-metallic ferromagnetic semiconductors (HMFS) by definition have only one spin component (either spin-up or spin-down) available for conduction, with the Fermi level crossing bands for only one spin orientation, and a band gap for the other spin orientation [1]. Such asymmetric electronic density of states for different spin channels at the Fermi level, in principle, means that electrical current in half-metallic materials can be completely spin polarised, and therefore HMFS materials are of considerable interest in spintronic device applications (such as memory devices and computer processors [2]) for injection and transport of highly spin polarised currents.

Half-metallic band structures have theoretically been predicted for certain ferromagnetic materials, mainly in Heusler alloys [3-5], among others [1], and were first experimentally confirmed in manganese perovskite [1]. In view of the potential application of HMFS materials in achieving spin-based electronic devices, substantial research efforts have been made towards understanding and improving the mechanisms of spin injection, transport and detection in this class of materials, but low Curie temperatures (T_C) and lack of other fundamental material properties [6] has remained a major challenge towards practical implementation in room temperature device applications. Therefore there is a need to explore new half-metallic ferromagnetic materials which may successfully be used for room temperature spintronic applications.

The prediction that the T_C of a Diluted Magnetic Semiconductor (DMS) scales with the host semiconductor's lattice constant a_0 as $1/a_0^3$ [7,8] makes diamond an excellent candidate for high T_C spintronic applications since it has the smallest lattice constant compared to all other known

[1]Author to whom correspondence should be addressed.

semiconductors. In addition, diamond is a promising material for many electrical and electronic applications due to its high electrical breakdown field and excellent thermal and electrical conductivities, compared to other semiconductors [9,10], which makes diamond an attractive material for the development of spin-based electronic devices in the emerging field of spintronics.

In this study, we report the energetic and magnetic ordering properties of Fe-doped diamond using *ab initio* pseudopotential DFT calculations, and show that diamond is likely to become a half-metallic ferromagnetic semiconductor which may be considered for high T_C spintronic device applications.

2. Computational details

The formation energy, stable structures and magnetic ordering properties of Fe in diamond, were modelled at various lattice sites and charge states, using *ab initio* pseudopotential Density Functional Theory, as implemented in the CASTEP code [11]. Formation energy and band structure calculations were carried out using a 64-atom diamond supercell constructed from $2 \times 2 \times 2$ conventional fcc diamond unit cells with an optimized lattice constant of 3.569 Å, in close agreement with the experimental value of 3.567 Å [12]. Full geometry optimization was performed without any symmetry or spin restrictions, with the Fe atom in various charge states (+2, +1, 0, -1, -2) placed at the divacancy, substitutional, tetrahedral interstitial or hexagonal interstitial lattice sites in a diamond supercell. For each lattice site and charge state, various initial positions of the Fe atom were considered, while the initial spin was systematically varied (from 0 μ_B to 6 μ_B) in order to determine the most stable geometries and spin states.

The Perdew-Burke-Ernzerhof generalized gradient approximation (GGA) [13] was used to treat the exchange-correlation effects of electron-electron interactions, together with Ultrasoft Vanderbilt pseudopotentials [14] incorporating non-linear core corrections [15,16] for the Fe atom.

A $4 \times 4 \times 4$ Monkhorst-Pack grid sampling [17] for integration over the Brillouin zone (32 *k*-points in the irreducible wedge of the Brillouin zone) was employed for spin and geometry optimization, with a planewave cut-off energy of 310 eV. Increasing the number of *k*-points or plane wave cut-off energy resulted in negligible changes in the total energy and structural relaxation effects (less than 10^{-4}eV and 10^{-3} Å, respectively).

In order to determine the energetically most favourable site of Fe in the diamond lattice as a function of charge state, the formation energy, E_f of Fe in the diamond supercell was calculated for each lattice site and charge state from

$$E_f^q = E_T^q - \sum_i n_i \mu_i + q\left(\varepsilon_V + \varepsilon_F\right),$$

where E_f^q is the total energy of the diamond supercell in a charge state q, while μ_i is the chemical potential of each atomic species, with n_i atoms per atomic species; ε_F is the Fermi energy measured relative to the energy of valence band maximum ε_V.

To predict the ground state magnetic ordering and other possible magnetic states in Fe-doped diamond, magnetic interactions were modelled using a 128 atom diamond supercell containing two Fe atoms (corresponding to an impurity concentration of 1.56 %) separated by an effective distance of two diamond lattice constants (7.138Å). For each charge state, different spin configurations corresponding to ferromagnetic, antiferromagnetic and nonmagnetic spin alignments of the Fe atoms were allowed so as to establish the most stable magnetic ordering and magnetic stabilization energies. Calculations of the energy differences between the different spin configurations and magnetic ordering were done using the final geometries obtained from the 64 atom supercellcalculations, using a well converged $4 \times 4 \times 2$ Monkhorst-Pack mesh of *k* points. Full geometry optimization using the enlarged 128 atom supercell in selected cases resulted in no changes in geometries or induced magnetic moments, with negligible changes in the magnetic stabilization energies (less than 0.01 meV). This approach has previously been used to successfully predict magnetic ordering in other semiconductors and oxides [18-22].

3. Results and discussion

3.1. Formation energy and stable charge states

The calculated formation energies of Fe for the most stable charge states in *p*-type (B-doped), and *n*-type (N- or P-doped) diamond at the divacancy and substitutional sites are summarized in table 1. At the interstitial sites (not shown), we find the formation energy of Fe to be considerably higher (by at least ~5 eV) compared to the substitutional or divacancy sites in any charge state [23], which makes it unlikely for interstitial Fe to be observed in diamond at equilibrium conditions. Importantly, we find the formation energy of Fe in diamond at any lattice site to be significantly dependent on the charge state (and hence the type of diamond doping), with the positive or negative charge states being significantly lower in energy in *p*-type and *n*-type diamond, respectively, compared to the neutral charge state.

We predict substitutional single positive Fe_S^{+1} and doubly positive iron Fe_S^{+2} to be the most favourable charge states in *p*-type diamond for Fermi energies close to the top of the valence band, while the substitutional neutral iron Fe_S^{0} is the most stable charge state in intrinsic diamond. In contrast, we find doubly negative iron at a divacancy Fe_{2V}^{-2} to be the most stable charge state in *n*-type diamond for Fermi energies ranging from the middle of the diamond band gap to the conduction band minimum (Table 1). This suggests that the most stable form of Fe in diamond is strongly dependent on the type of diamond doping (intrinsic, *p*-type or *n*-type), and therefore on the position of the Fermi level as influenced by other impurities (such as boron, nitrogen or phosphorus) in diamond.

Table 1: Formation energies and optimized point symmetries of Fe in different charge states (+2, +1, 0, −1, −2), together with carbon nearest neighbour (C_{NN}) distortions at divacancy and substitutional lattice sites in diamond. Numbers in brackets indicate the multiplicity of each Fe-C_{NN} distortion. C_1 indicates a relaxation with no unique symmetry. Formation energies are given in *p*- and *n*-type diamond, with Fermi levels pinned to acceptor or donor levels of boron (Ev + 0.37 eV, *p*-type), as well as nitrogen (E_c − 1.6 eV, *n*-type) or phosphorus (E_c − 0.6 eV, *n*-type), respectively. Lowest formation energies at each lattice site in each type of doped diamond are indicated in bold.

	Formation energy, E_f(eV)			Symmetry	Fe-C_{NN} distortion (Å)	Fermi energy (eV)
	B-doped	N-doped	P-doped			
(a) Divacancy Fe						
Fe^{+2}	6.42	13.46	15.46	D_{3d}	0.10(6)	-
Fe^{+1}	**6.04**	9.56	10.56	C_2	0.24(2), 0.09(2), -0.05(2)	0.00 - 0.87
Fe^{0}	6.54	6.54	6.54	C_1	0.20(2), 0.07, 0.06, -0.050(2)	0.87 - 2.46
Fe^{-1}	8.90	5.38	4.38	D_{3d}	0.05(6)	-
Fe^{-2}	10.72	**3.68**	**1.68**	D_{3d}	0.04(6)	2.46 - 5.49
(b) Substitutional Fe						
Fe^{+2}	**5.62**	12.66	14.66	T_d	0.22(4)	0.00 - 0.37
Fe^{+1}	**5.62**	9.14	10.14	T_d	0.21(4)	0.37 - 0.98
Fe^{0}	6.23	**6.23**	6.23	T_d	0.19(4)	0.98 - 4.64
Fe^{-1}	10.50	6.98	**5.98**	C_{3v}	0.20(3), 0.94	4.64 - 4.89
Fe^{-2}	15.25	8.21	6.21	T_d	0.21(4)	4.89 - 5.49

3.2. Magnetic interaction

We find substitutional Fe_S^{+1} and Fe_S^{+2} iron, which are the energetically most stable charge states in *p*-type diamond, order ferromagnetically with significant magnetic moments of 1.0 μ_B and 1.8 μ_B per atom, and ferromagnetic stabilization energies (ΔE) of 33.3 meV and 7.5 meV, respectively. On the other hand, we find the spin interactions in divacancy iron Fe_{2V}^{-2}, which is the most stable charge state in *n*-type diamond, to be antiferromagnetic, with the ferromagnetic spin state being higher in energy by 1.7 meV compared to the antiferromagnetic spin state. In intrinsic diamond, however, we find the most stable charge state, substitutional iron Fe_S^0, to be non-magnetic.

Since the achievable Curie temperature in a DMS is proportional to its ferromagnetic stabilization energy, $\Delta E = E_{FM} - E_{AF}$ [24], our results therefore indicate that substitutional iron in the single positive charge state Fe_S^{+1} may order ferromagnetically in *p*-type diamond at significantly larger Curie temperatures compared to other transition metals in diamond which have been considered so far [25,26].

To assess the spin character of the impurity bands at the Fermi level in Fe-doped diamond, Figure 1 shows the calculated spin-up and spin-down band structures of ferromagnetic Fe^{+1} doped-diamond at the substitutional site, while Figure 2 illustrates the corresponding spin polarised partial density of states, showing the contribution from Fe and the sum of carbon orbitals to the impurity bands, respectively. It is evident that incorporation of Fe^{+1} into diamond induces strongly spin-polarised impurity bands into the diamond band-gap, while maintaining the semiconducting property of diamond. These impurity bands are seen to originate from *s,p-d* hybridization between carbon 2*s*, 2*p* and Fe 3*d* orbitals. In addition, we find that the Fe 4*p* orbitals also make a significant contribution to the unoccupied spin-up and spin-down bands in the middle of the band gap, though they are absent from the partly occupied spin-down bands lower in the band gap.

Interestingly, the Fermi level in substitutional Fe_S^{+1}-doped diamond crosses bands in only one spin channel, the spin-down bands. Consequently, electrons at the Fermi level will be exclusively spin-down polarized, with the spin-up band acting as an insulator for the spin-up electrons, indicating that substitutional Fe^{+1}-doped diamond is a half-metallic ferromagnetic semiconductor. This is particularly significant for efficient spin injection of spin polarized current in spintronic device applications, since charge carriers travelling at the Fermi surface will undergo 100% spin polarisation.

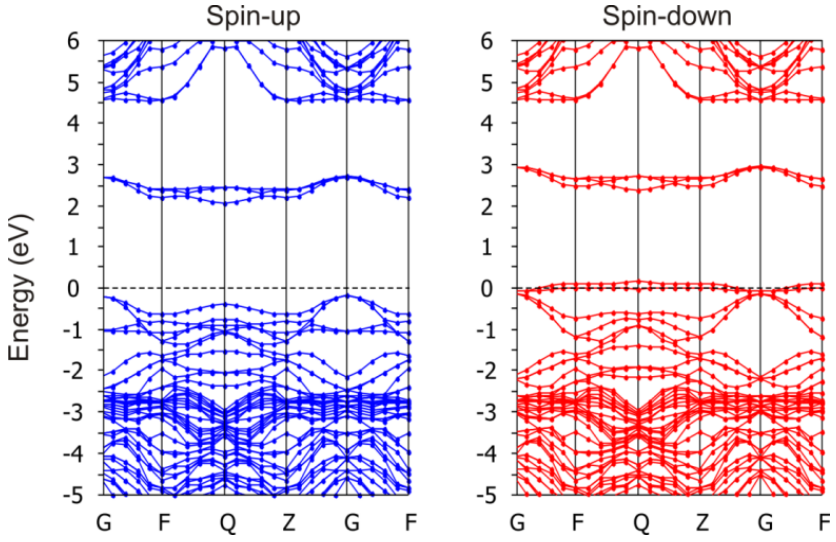

Figure 1: Spin-up and spin-down band structures of Fe^{+1} doped diamond illustrating half-metallicity of states at the Fermi level. Energies are relative to the respective Fermi levels, shown with horizontal dashed lines. Dots correspond to data points; lines guide the eye.

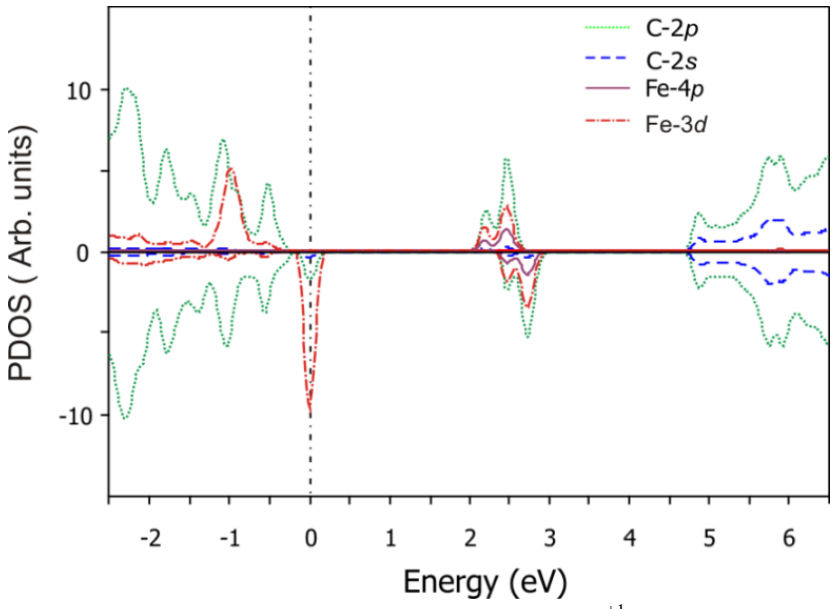

Figure 2: Partial density of states (PDOS) of substitutional Fe^{+1} in diamond. All energies are relative to the Fermi energy shown with the vertical dashed line.

4. Conclusion

The energetic stability and magnetic ordering properties of Fe-doped diamond have been investigated using *ab initio* pseudopotential DFT calculations at various charge states and lattice sites. We find the formation energy of Fe in diamond at any lattice site to be significantly dependent on the charge state and hence the type of diamond doping (intrinsic, *n*-type or *p*-type), with the positive or negative charge states having lower formation energies in *p*-type and *n*-type diamond, respectively, compared to the neutral charge state. Similarly, the magnetic properties of Fe-doped diamond are also strongly dependent on the charge state and the type of diamond doping, and therefore on the position of the Fermi level in the diamond band gap as influenced by other impurities (such as boron, nitrogen or phosphorus) in diamond samples.

We predict substitutional Fe_S^{+1} and Fe_S^{+2} to be the most favourable charge states in *p*-type diamond for Fermi energies close to the top of the valence band, while divacancy Fe_{2V}^{-2} is the most stable charge state in *n*-type diamond for Fermi energies ranging from the middle of the diamond band gap to the conduction band minimum. Importantly, we find that substitutional Fe_S^{+1} orders ferromagnetically in diamond with a magnetic moment of 1.0 μ_B and a large ferromagnetic stabilization energy of 33.3 meV. The impurity bands at the Fermi level exhibit a half-metallic character, with the Fermi level crossing bands in only the spin-down bands, indicating that substitutional Fe^{+1}-doped diamond is a half-metallic ferromagnetic semiconductor which islikely to order ferromagnetically with higher Curie temperatures, than has previously been achieved in other semiconductors [24]. In addition, we have subsequently shown [27] that the interaction remains strongly ferromagnetic at all the Fe-Fe separations considered (up to two lattice constants), while some clustering of Fe atoms may occur after high temperature annealing.

5. References

[1] Katsnelson M I, Irkhin V Y, Chioncel L, Lichtenstein A I and R.A. de Groot 2008 *Rev. Mod. Phys*. **80** 315
[2] Awschalom D D and Kikwaka J 1999, *Phys. Today* 33
[3] Picozzi S, Continenza A and Freeman A J 2002 *Phys. Rev.* B **66** 094421
[4] Galanakis I 2005 *Phys. Rev.* B **71** 012413
[5] Wurmehl S, Fecher G H, Kandpal H C, Ksenofontov V, Felser C and Lin H-J 2006 *Appl. Phys.*

Lett. **88** 032503
[6] Wolf S A, Awschalom D D, Buhrman R A, Daughton J M, von Molnar S, Roukes M L, Chatcehlkanova A Y and Treger D M 2001 *Science* **294** 1488
[7] Dietl T, Ohno H, Matsukura F, Cibert J and Ferrand D 2000 *Science* **287** 1019
[8] Dietl T, Ohno H and Matsukura F 2001 *Phys. Rev.* B **63** 195205
[9] Wort J H and Balmer R S 2008 *Mater. Today* **11** 22
[10] Kalish R, 2007 *J. Phys. D: Appl. Phys* **40** 6467
[11] Clark S J, Segall M D, Pickard C J, Hasnip P J, Probert M J, Refson K and Payne M C 2005 *Zeitschrift fuer Kristallographie* **220** 567
[12] Donnay J D H and Ondik H M 1973 *Crystal Data: Determinative Tables Vol. 2, 3rd ed.* (US Department of Commerce - National Bureau of Standards - JCPDS)
[13] Perdew J P, Burke K and Ernzerhof M 1996 *Phys. Rev. Lett.* **77** 3865
[14] Vanderbilt D 1990 *Phys. Rev.* B **41** 7892
[15] Fabris S, de Girancoli S, Baroni S, Vicario G and Balducci G 2005 *Phys. Rev.* B **72** 237102
[16] Fabris S, de Gironcoli S, Baroni S, Vicario G and Balducci G 2005 *Phys. Rev.* B **71** 041102(R)
[17] Monkhorst H J and Pack J D 1976 *Phys. Rev.* B **13** 5188
[18] Kronik L, Jain M and Chelikowsky J R 2002 *Phys. Rev.* B **66** 041203
[19] Pardo V, Blaha P, Iglesias M, Schwarz K, Baldomir D and Arias J E 2004 *Phys. Rev.* B **70** 144422
[20] Osuch K, Lombardi E B and Adamowicz L 2005 *Phys. Rev.* B **71** 165213
[21] Osuch K, Lombardi E B and Gebicki W 2006 *Phys. Rev.* B **73** 075202
[22] Los A and Los V 2010 *J. Phys.: Condens. Matter* **22** 245801
[23] Benecha E M and Lombardi E B *in Proceedings of SAIP 2011, the 56th Annual Conference of the South African Institute of Physics*, p 20 ISBN: 978-1-86888-688-3
[24] Sato K, Schweika W, Dederichs P H and Yoshida H K 2000 *Phys. Rev.* B 70 201202(R)
[25] Benecha E M and Lombardi E B 2011 *Phys. Rev.* B **84** 2352001
[26] Lombardi E B 2008 *Diamond Rel. Mater.* **17** 1345
[27] Benecha E M and Lombardi E B 2013 *J. Appl. Phys.* **114** 223703